Transmission Electron Microscopy of Centrioles, Basal Bodies and Flagella in Motile Male Gametes of Land Plants

Karen Sue Renzaglia*, Renee A. Lopez, Jason S. Henry, Nicholas D. Flowers and Kevin C. Vaughn[$]

Department of Plant Biology, Southern Illinois University, Carbondale, IL, USA
*For correspondence: renzaglia@siu.edu
[$]Retired

[Abstract] Motile male gametes (spermatozoids) of land plants are coiled and contain a modified and precisely organized complement of organelles that includes a locomotory apparatus with two to thousands of flagella. Each flagellum is generated from a basal body that originates *de novo* as a centriole in spermatogenous cell lineages. Much of what is known about the diversity of plant male gametes was derived from detailed transmission electron microscopic studies. Because the process of spermatogenesis results in complete transformation of the shape and organization of these cells, TEM studies have yielded a wealth of information on cellular differentiation. Because green algal progenitor groups contain centrioles and a variety of motile cells, land plant spermatozoids also provide a plethora of opportunities to examine the evolution and eventual loss of centrioles and locomotory apparatus during land colonization.

Here we provide a brief overview of the studies and methodologies we have conducted over the past 20 years that have elucidated not only the structural diversity of these cells but also the development of microtubule organizing centers, the *de novo* origin of centrioles and the ontogeny of structurally complex motile cells.

Keywords: Blepharoplast, Basal bodies, Centrioles, Extracellular matrix, Flagella, Transmission electron microscopy

[Background] Motile gametes of land plants are strikingly diverse and develop through transformations that involve repositioning, and reshaping of cellular components, and the assembly of a complex locomotory apparatus (Renzaglia and Garbary, 2001; Lopez and Renzaglia, 2008). Because of constraints imposed by cell walls, elongation of the cell and flagella is around the periphery of a nearly spherical space, resulting in a coiled configuration of the mature gamete (Renzaglia and Garbary, 2001; Lopez and Renzaglia, 2014). The degree of coiling varies from just over one to as many as 10 revolutions per cell. The number of flagella per gamete is even more variable, ranging from two in bryophytes (mosses, hornworts, liverworts and most lycophytes) to an estimated 1,000-40,000 in *Ginkgo* and cycads, the earliest divergent seed plant lineages. Following the diversification of *Ginkgo* and cycads, all vestiges of basal bodies and flagella were lost in the remaining seed plants that utilize pollen tubes to deliver non-motile sperm to egg cells (Southworth and Cresti, 1997).

It is widely known that vegetative plant cells lack centrioles and the centrosome is elusive. A lesser-known fact is that in plants with motile sperm cells, centrioles arise *de novo* during the penultimate or

![bio-protocol logo]

ultimate mitotic divisions that produce the nascent spermatid in antheridia (Renzaglia and Carothers, 1986; Vaughn and Renzaglia, 1998; Vaughn and Harper, 1998; Renzaglia and Maden, 2000; Vaughn and Renzaglia, 2006). In these cell lineages, centriolar centrosomes serve as the nucleation site for spindle microtubules and thus bear striking parallels with centrioles of animal and protist cells. In the developing sperm cells, the centrioles reposition, anchor to form the distinctive basal bodies, and elongate to produce the 2-40,000 flagella in each gamete. These changes occur in synchrony with cell elongation, and the entire process of cytomorphogenesis is guided by the production of unique arrays of microtubules, and fibrillar and lamellar bands or strips. Because of the exclusive occurrence of basal bodies, flagella and associated complexes in developing male gametes, studies of spermatogenesis have revealed important information on the structure, composition, and developmental changes in microtubule arrays as they relate to the cell cycle, microtubule organizing centers (MTOCs), and cellular differentiation in plants. The purpose of this review is to describe the method used in transmission electron microscopic examination and to demonstrate how this approach has advanced understanding of basal bodies, flagella/cilia, and associated structures in land plants.

Materials and Reagents

A. Transmission electron microscope (TEM)
　1. Scintillation vials with aluminum covered caps (Fisher Scientific, catalog number: 03-340-4B)
　　Manufacturer: DWK Life Sciences, Kimble®, catalog number: 7450320.
　2. BEEM embedding capsules size '00' (Electron Microscopy Sciences, catalog number: 70000-B)
　3. Formfar Carbon Film 200 mesh Ni grids (Electron Microscopy Sciences, catalog number: FCF200-Ni)
　4. Copper 200 mesh grids (Electron Microscopy Sciences, catalog number: EMS200-Cu)
　5. Sperm cells
　　a. *Megaceros flagellaris*
　　b. *Phaeoceros carolinianus*
　　c. *Phylloglossum drummondii*
　　d. *Ginkgo biloba*
　　e. *Angiopteris evecta*
　　f. *Conocephalum conicum*
　　g. *Ceratopteris richardii*
　　h. *Riccardia multifida*
　　i. *Aulacomnium palustre*
　　j. *Equisetum arvense*
　6. Ethanol (Decon Labs, catalog number: 2705HC)
　7. Low viscosity resin
　8. Glutaraldehyde (Electron Microscopy Sciences, catalog number: 16120)

9. Sorensens phosphate buffer, 0.2 M, pH 7.2 (Electron Microscopy Sciences, catalog number: 11600-10)

10. Osmium tetroxide (Electron Microscopy Sciences, catalog number: 19150)

11. Potassium ferrocyanide (Fisher Scientific, catalog number: P236-500)

12. Uranyl acetate (Polyscience, catalog number: 21447-25)

13. 100% methanol

14. Lead nitrate (Electron Microscopy Sciences, catalog number: 17900)

15. Sodium citrate (Electron Microscopy Sciences, catalog number: 21140)

16. 1 N NaOH

17. 100% propylene oxide (Electron Microscopy Sciences, catalog number: 20401)

18. 2.5% glutaraldehyde (see Recipes)

19. 0.05 M phosphate buffer (pH 7.2) (see Recipes)

20. 4% aqueous osmium tetroxide (see Recipes)

Equipment

A. Transmission electron microscope (TEM)
   1. Diamond knife (Diatome, specs: Ultra, 45°, 4 mm, Wet)
   2. Transmission electron microscope (Hitachi, model: HF7100)

Procedure

A. Transmission electron microscope (TEM)

TEM examination has revealed diagnostic developmental features and structural peculiarities of plant spermatozoids. Three examples that illustrate these plant specific features are superficially described herein: basal body origin (Figure 1), locomotory apparatus development (Figure 2) and basal body/flagella structure (Figure 3). The *de novo* appearance of basal bodies takes several unique forms, the most notable of which are bicentrioles and blepharoplasts. Sperm cells of bryophytes and most lycophytes are biflagellated and in these plants, basal bodies originate as two centrioles attached end to end (Figure 1A). Centrioles have the typical complement of nine overlapping triplet microtubules around a central core or hub (Figure 1B). Each nascent sperm cell inherits one bicentriole and during development, the two centrioles separate, reposition and become the basal bodies in the biflagellate gametes. In ferns, blepharoplasts form in spermatogenous cells. Each blepharoplast is spherical and contains the central hubs of all basal bodies in a dense matrix that will be assembled in the young spermatid (Figure 1C).

An alternate mode of origin of centrioles occurs in *Phylloglossum*, one of two lycophytes with multiple flagella. In this case, the centrioles originate as a branched unit of central hubs on to which the triplets assemble directly (Figure 1D). The 20 or so basal bodies formed this way separate and align around the anterior of the developing spermatid and elongate into the flagella. In the seed plant,

Ginkgo biloba, a pair of massive blepharoplasts in the sperm mother cell assembles approximately 1,000 centrioles around an electron dense unit that contains spherical electron lucent areas occasionally containing basal bodies (Figure 1E). The cycads produce a blepharoplast similar to that of *Ginkgo*, but much larger, producing an estimated 40,000-50,000 basal bodies (Gifford and Larson, 1980).
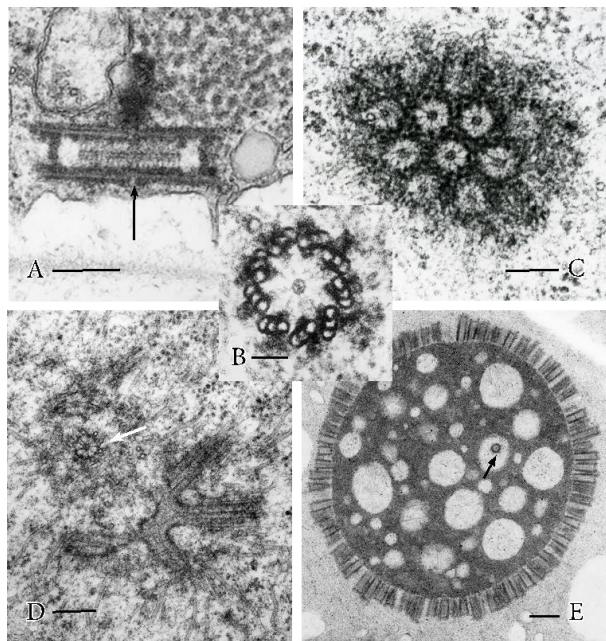

Figure 1. Origin of basal bodies in spermatogenous cells. A. The bicentriole of bryophytes and most lycophytes is represented here in *Megaceros flagellaris*, a hornwort. It consists of two centrioles attached end-to-end by a central core (arrow). B. Cross section of a bicentriole of *Phaeoceros carolinianus*, a hornwort, showing the nine triplets in the centriole/basal body arranged around a central core or hub. C. The blepharoplast of ferns as illustrated in *Ceratopteris richardii* contains numerous basal body hubs embedded in an amorphous dense matrix. D. A pair of branched centriolar units forms in the spermatid mother cell of *Phylloglossum drummondii*, one of two lycophytes with approximately 20 flagella. Triplet microtubules are assembled directly on the hub with A microtubules produced first (arrow) followed by B and C microtubules. E. A massive blepharoplast in the sperm mother cell of *Ginkgo biloba* has approximately 1,000 centrioles around an electron dense unit that contains spherical electron lucent areas occasionally containing basal bodies (arrow). Bars = 0.2 µm (A, C, D), 0.1 µm (B), 1.0 µm (E).

In the nascent spermatid, basal bodies separate and migrate as other elements of the locomotory apparatus develop. This repositioning is often in association with a dense microtubule-organizing center from which numerous microtubules emanate (Figure 2A). In ferns, basal bodies are assembled around the central hubs as A, B, and C microtubules of the triplets are added (Figure 2B). Then the short basal bodies migrate in concert with construction of the multilayered structure,

composed of a lamellar strip and band of microtubules (Figure 2C), until they are positioned around the anterior coils of the cell in a precise arrangement (Figure 2D). While repositioning, basal bodies begin to elongate from both ends. At the proximal end, more triplets are added to elongate the basal body and in ferns the hub forms a highly elongated extension that is transient and disappears in the late stage spermatozoid (Figure 2E). A transition zone (Figure 2E) that contains the stellate configuration begins formation during basal body repositioning (Figure 2D).
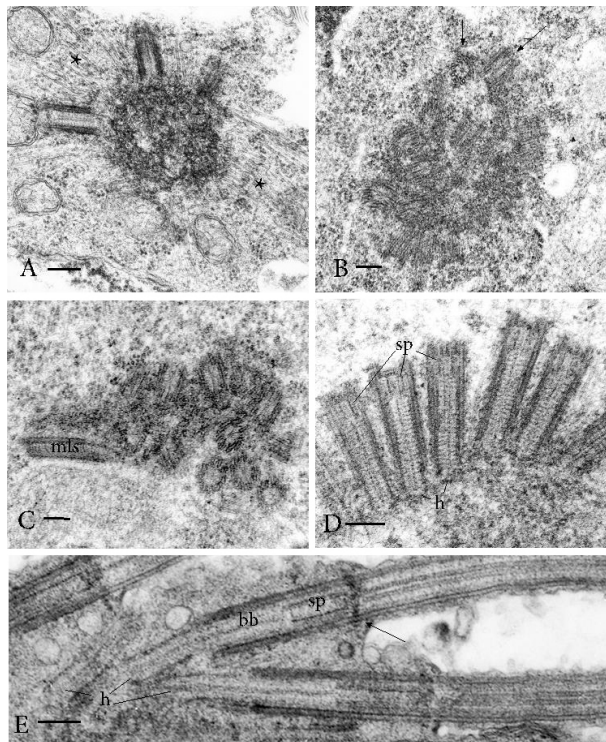
Figure 2. Microtubule-organizing centers and development of the locomotory apparatus in spermatids (developing sperm cells). A. Dense microtubule-organizing center (MTOC) with emanating microtubules (*) and three basal bodies in *Phylloglossum drummondii*. The MTOC guides basal body placement. B. In spermatids of *Ceratopteris richardii*, short basal bodies seen in cross section (left arrow) and longitudinal section (right arrow) are developing and reorganized in an electron-dense matrix. C. The reorganization of basal bodies in *C. richardii* occurs in synchrony with the development of a multilayered structure (mls) that is composed of a lamellar strip and band of microtubules. D. During the assembly of the anterior locomotory apparatus, the basal bodies of *C. richardii* grow from both ends resulting in neatly aligned elongated basal bodies; the posterior transition region with a stellate pattern (sp) is beginning to elongate in these basal bodies. E. Long hub extensions (h) in *Angiopteris evecta*, a eusporangiate fern, are visible after the flagella initiate elongation but prior to completion of sperm cell differentiation. The extensions are transient and thus are lacking in the mature gamete. Basal bodies (bb) and the stellate pattern (sp) in the transition region are located internal to emergence of flagella from the cell body (arrow). Bars = 0.2 μm (A-E).

www.bio-protocol.org/e2448

Proximal basal body elongation is critical in positioning basal bodies in mosses and liverworts spermatozoids that have two dimorphic, staggered basal bodies (Figures 3A-3C). Staggering is achieved by proximal elongation of usually three ventral triplets in one basal body that becomes very long (Figure 3A) and is eventually anchored some distance from the less elongated anterior basal body. Slight proximal elongation of dorsal triplets in the anterior basal body anchors it within the multilayered structure (Figure 3B). A peculiar feature of moss gamete development is the existence of a single microtubule that strays from the microtubular band and appears to guide the ventral triplets into position during elongation of the posterior basal body (Figure 3C).
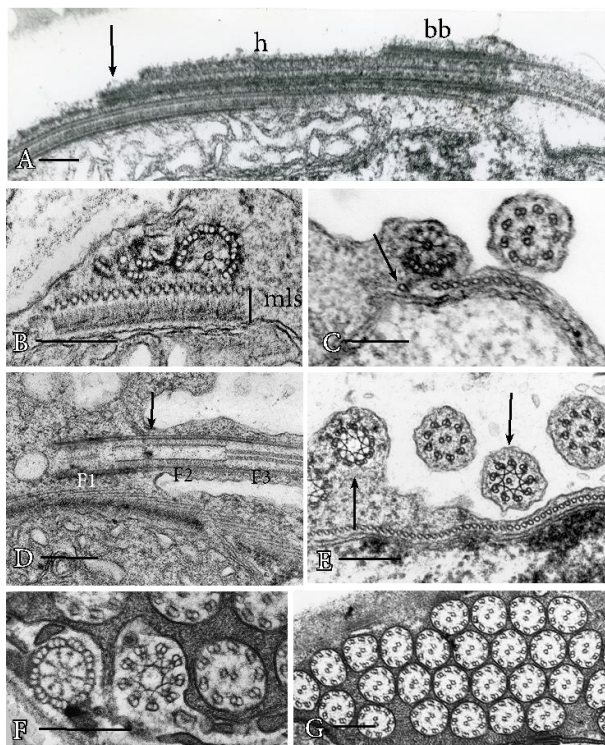
Figure 3. Structure of mature basal bodies and flagella. A. Posterior basal body of *Riccardia multifida*, a simple thalloid liverwort, consists of elongated ventral triplets (arrow) and hub (h) that extend well beyond the original basal body (bb). B. Dimorphic basal bodies of *Conocephalum,* a complex thalloid liverwort, in cross section. The multilayered structure (mls) subtends an anterior basal body on the right with hub and six triplet extensions and posterior basal body on the left that consists solely of three ventral triplet extensions. C. The posterior basal body of mosses, illustrated in *Aulacomnium palustre*, consists of a hub and three ventral triplet extensions that connect to and are guided to their final position by a single stray microtubule (arrow). Visible in this cross section is the anterior flagellum on the right just exterior to the band of microtubules of the multilayered structure. D. Longitudinal section of basal bodies and flagella in the lycophyte *Phylloglossum*, illustrating the basal body (F1), transition zone (F2) and flagellum (F3) that correspond to the cross sections from right to left in figure F in *Equisetum*. Notably, the stellate pattern of the transition zone is located anterior and posterior to the emergence of the flagellum from the cell body (arrow). E. Cross section of two basal bodies at

the stellate pattern of the transition region and two flagella in *Phylloglossum*. The stellate pattern (left arrow) that is still contained in the cell body consists of nine overlapping triplets and the one that is in the flagellar shaft (right arrow) has nine overlapping doublets with a single central microtubule. F. Cross sections of basal body, stellate pattern and axoneme at the levels indicated as F1, F2 and F3 in figure D. G. Cross sections of flagella in *Ceratopteris* demonstrating the typical 9+2 configuration of land plant axonemes. Bars = 0.2 μm (A-F).

Note: For each solution change below, completely saturate tissue by adding solution until it rises over the material in the vial/ tube (this could be anywhere from 1 ml to 5 ml (or more) of solution depending on how much tissue is in each tube or vial).

1. Fix antheridial tissue (either excised or whole gametophytes if very small *e.g.*, *Ceratopteris* fern male gametophytes) in 2.5% glut in 0.05 M sodium phosphate buffer (pH 7.2).

2. Rinse three times (15 min each) in 0.05 M phosphate buffer (pH 7.2).

3. Post-fix for 2 h at room temperature in aqueous 2% osmium tetroxide (optional with 1.5% potassium ferrocyanide).

4. Rinse three times in double distilled autoclaved water (10 min each), dehydrated through 25%, 50%, 75% and 95% ethanol (20 min each), rinsed twice in 100% ethanol (20 min each), then rinse three times in 100% propylene oxide (15 min each).

5. Infiltrate in 25%, 50% and 75% in low viscosity resin (diluted with propylene oxide) for 12 h each at 4 °C and soaked in three changes of pure resin for 8 h each.

6. Place one or two antheridia (depending on size) per BEEM embedding capsule and polymerize in oven for 48 h at 60 °C.

7. Cut gold/silver sections with a diamond knife, and collect on either formvar films using slot (1 x 2 mm) or on 200 mesh copper grids.

8. Post-stain with 2% uranyl acetate (2 min) followed by basic lead citrate (5 min) prior to viewing in a Hitachi HF7100.

Recipes

1. 0.01 M phosphate buffer (pH 7.2)
   Add 5 parts 0.20 M Sorenson's phosphate buffer (pH 7.2) to 95 parts double distilled autoclaved water

2. 0.05 M phosphate buffer (pH 7.2)
   Add 25 parts 0.20 M Sorenson's phosphate buffer (pH 7.2) to 75 parts double distilled autoclaved water

3. 2.5% glutaraldehyde
   a. Add 1 part 10% glutaraldehyde to 1 part double distilled autoclaved water
   b. Add 1 part 0.20 M Sorensen's phosphate buffer (pH 7.2) to 1 part double distilled autoclaved water

  c. Add 1 part 5% glutaraldehyde to 1 part 0.10 M Sorensen's phosphate buffer (pH 7.2)

4. 0.05 M sodium cacodylate buffer (pH 7.2)

  Add 1 part 0.30 M sodium cacodylate buffer (pH 7.2) to 6 parts double distilled autoclaved water

5. 2% aqueous osmium tetroxide

  Add 1 part 4% aqueous osmium tetroxide to 1 part double distilled autoclaved water

6. 0.02 M phosphate buffer (pH 7.2)

  Add 1 part 0.20 M Sorenson's phosphate buffer (pH 7.2) to 10 parts double distilled autoclaved water

7. 0.05 M PIPES buffer (pH 7.2)

  Add 1 part 0.30 M PIPES buffer (pH 7.2) to 6 parts double distilled autoclaved water

8. 1.5% potassium ferrocyanide

  Add 1.5 g potassium ferrocyanide to 10 ml double distilled autoclaved water

9. 2% uranyl acetate

  Add 2 g uranyl acetate to 10 ml double distilled autoclaved water or 100% methanol

10. Reynold's lead citrate

  a. Add 1.33 g lead nitrate and 1.76 g sodium citrate to 30 ml boiled double distilled autoclaved water that has cooled to room temperature and shake for 30 min

  b. Add 8 ml 1 N NaOH

  c. Add 12 ml double distilled autoclaved water

Acknowledgments

References

1. Gifford, E. M. and Larson, S. (1980). Developmental features of the spermatogenous cell in *Ginkgo biloba.* *Am J Bot* 62: 119-124.

2. Lopez, R. A. and Renzaglia, K. S. (2008). Sperm cell architecture, insemination, and fertilization in the model fern, *Ceratopteris richardii.* *Sex Plant Reprod* 21: 153-167.

3. Lopez, R. A. and Renzaglia, K. S. (2014). Multiflagellated sperm cells of *Ceratopteris richardii* are bathed in arabinogalactan proteins throughout their development. *Am J Bot* 101: 2052-2061.

4. Renzaglia, K. S. and Carothers, Z. B. (1986). Ultrastructural studies of spermatogenesis in the Anthocerotales. IV. The blepharoplast and mid-stage spermatid of *Notothylas.* *J Hattori Bot Lab* 60: 97-104.

5. Renzaglia, K. S. and Garbary, D. J. (2001). Motile male gametes of land plants: Diversity, development, and evolution. *Crit Rev Sci* 20:107-213.

6. Renzaglia, K. S. and Maden, A. R. (2000). Microtubule organizing centers and the origin of centrioles during spermatogenesis in the pteridophyte *Phylloglossum. Micros Res Tech* 49: 496-505.

7. Southworth, D. and Cresti, M. (1997). Comparison of flagellated and nonflagellated sperm in plants. *Am J Bot* 84: 1301-1311.

8. Vaughn, K. C. and Harper, J. D. (1998). Microtubule-organizing centers and nucleating sites in land plants. *Int Rev Cytol* 181: 75-149.

9. Vaughn, K. C. and Renzaglia, K. S. (1998). Origin of bicentrioles in anthocerote spermatogenous cells. In Bates, J. W., Ashton, N., Duckett, J. G. (Eds.). Bryology for the Twenty-First Century.

10. Vaughn, K. C. and Renzaglia, K. S. (2006). Structural and immunocytochemical characterization of the *Ginkgo biloba* L. sperm motility apparatus. *Protoplasma* 22: 165-173.